

Optical functions of silicon between 1.7 and 4.7 eV at elevated temperatures

G. E. Jellison, Jr. and F. A. Modine

Solid State Division, Oak Ridge National Laboratory, Oak Ridge, Tennessee 37830

(Received 6 December 1982)

Polarization modulation ellipsometry has been used to determine the optical functions of silicon at elevated temperatures up to 1000 K. The E_1 , E'_0 , and E_2 features move monotonically to lower energies as the temperature is increased. A fit of the E'_0 and E_2 peak positions to the empirical formulation of Varshni is obtained; it is found that the critical points of the joint density of states for the E'_0 and E_2 gaps move somewhat differently from the indirect gap, although the difference is not large.

I. INTRODUCTION

Accurate knowledge of the optical functions of silicon at elevated temperatures is extremely important for many applications, including melting-model calculations of pulsed laser annealing,¹ concentrator solar cell applications,² the interpretation of Raman temperature measurements,³⁻⁵ and the determination of the positions of critical points in the Brillouin zone as a function of temperature. Though the optical data for silicon is extensive at and below room temperature,⁶⁻¹² much less data exists for elevated temperatures. Several authors have reported the temperature dependence of the complex index of refraction at the He-Ne laser line [632.8 nm (Refs. 13-15)], and Weakliem and Redfield¹⁶ have determined the optical-absorption coefficient (α) from room temperature to 200°C and from 1.1 to 2.7 eV using optical transmission measurements. Macfarlane *et al.*¹⁷ also used optical transmission measurements to determine α at low photon energies (less than 1.2 eV) for temperatures between 4.2 and 415 K, while Compaan and Lo have reported¹⁸ α at 300, 650, and 900 K at three common argon-ion laser lines (457.9, 488.0, and 514.5 nm). A detailed analysis of the temperature dependence of the optical absorption at the He-Ne infrared laser line (1.152 μm) by Jellison and Lowndes¹⁹ shows that the formulation by Macfarlane *et al.*¹⁷ is correct at that wavelength for temperatures up to ~ 1150 K. The wavelength dependence of the complex dielectric constant has been reported by Daunois and Aspnes¹⁰ at 10 and 300 K and by Aspnes and Theeten¹¹ at 300 K. Similar measurements have been made recently by Jellison and Modine¹² at 10 and 300 K.

The theoretical aspects of the temperature-dependent optical properties have recently been reviewed by Cohen and Chadi.²⁰ The main thrust of the theoretical calculations has focused on calculat-

ing the energy change at various critical points of the Brillouin zone as a function of temperature. Three major approaches to the temperature dependence of semiconductor band gaps have been employed: The first approach, used by Fan,²¹ incorporates the temperature dependence into an electron self-energy term. The second approach, used by Antonchik²² and later Brooks and Yu,²³ incorporates the temperature dependence by including a Debye-Waller factor in the structure factor of a pseudopotential calculation. The third approach, used by Brooks²⁴ and later by Heine and Van Vechten,²⁵ describes the effect of temperature by considering the effect of the electrons on the phonons. In a more recent paper, Allen and Cardona²⁶ calculated the temperature dependence of the E_0 direct gap in Ge by including both the Debye-Waller factor and the self-energy term. They found that the inclusion of both factors improved the agreement with experiment (minus thermal expansion), but more terms need to be taken into account for a truly accurate theoretical description.

This paper presents the optical functions of silicon determined with the use of polarization modulation ellipsometry (PME) between 1.65 and 4.77 eV in the temperature range from 10 to 972 K. We also extend the preceding work in which we reported accurate determinations of the optical functions at 10 and 300 K,¹² and of α as a function of temperature.²⁷ Details of the experimental system and the data analysis are described with respect to the difficulties encountered in performing high-temperature PME measurements in Sec. II. The resulting values of the dielectric functions are presented in Sec. III, where we show that the E'_0 and E_2 features of the dielectric functions move monotonically to lower photon energy as the temperature is increased and that the shift is well described by the empirical formulation of Varshni.²⁸

II. EXPERIMENTAL METHODS AND DATA ANALYSIS

Ellipsometry data were taken as a function of temperature and wavelength by using the polarization modulation ellipsometer and procedures that have been described in detail elsewhere.¹² Here we describe only the procedures used to perform high-temperature measurements.

There are two major problems associated with the performance of high-temperature ellipsometric measurements on silicon. Firstly, the oxidation rate of the Si surface increases exponentially with temperature; the solution to this problem is discussed in Ref. 27. Briefly, we enclosed the sample in a stainless-steel chamber which was closed except for small optical ports that allow light to enter and exit without passing through windows. The chamber was over-pressured with forming gas (4% H₂, 96% Ar) to reduce surface oxidation. The ellipsometry measurements indicated minimal (less than 4 Å) additional oxide growth at high temperatures.

Secondly, the sample itself acts as a light source at high temperature, with the total emittance increasing as T^4 and the peak of the emission shifting toward the visible [$E_{\text{max}}(\text{eV}) = 4.29 \times 10^{-4} T(\text{K})$]. Sample emission rapidly becomes a problem as the temperature is increased. Because the customary ellipsometer arrangement was used (with the monochromator between the light source and the sample), data could be taken only up to 1000 K before this background emission became intolerable.

In order to obtain data at temperatures approaching 1000 K, it was necessary to reduce the emission reaching the phototube and to make corrections to the data taken at the highest temperatures. Since at 1000 K the sample emission peaks in the infrared (0.43 eV), it was possible to considerably reduce the emission problem by changing to a photomultiplier tube with an S-10 cathode (EMI 95921B), which has a relatively poor infrared response. This permitted meaningful measurements to be made over the visible portion of the spectrum. In the ultraviolet (greater than or equal to 3.0 eV), where the light source (xenon arc lamp) becomes much weaker, it was necessary to further reduce the emission reaching the phototube by judicious use of high-pass optical filters.

The data consisted of signals proportional to $\cos(2\psi)$ and $\sin(2\psi)\sin(\Delta)$ which were measured in configurations I and III, respectively.¹² Because the ellipsometer is a photometric instrument which operates in a constant dc current mode, the signals were reduced by sample emission in direct proportion to the fraction of the light that is contributed by the emission. Thus the effect of the emission on

the measurements is described by

$$S' = \frac{F_0 S}{F_0 + F_e}, \quad (1)$$

where S' and S denote the reduced and true magnitudes of the signal, and F_0 and F_e denote the effective light flux contributed by the ellipsometer source and the sample emission, respectively.

The signal reduction due to sample emission was determined as a function of wavelength by comparing the phototube voltage with and without the light flux contributed by the ellipsometric source. For an n -stage photomultiplier tube operated in a constant current mode, the n th power of the phototube voltage is inversely proportional to the light flux; thus

$$\frac{F_0}{F_0 + F_e} = 1 - \frac{F_e}{F_0 + F_e} = 1 - \left[\frac{V}{V_e} \right]^n, \quad (2)$$

where V (V_e) represents the phototube voltages measured with (without) the contribution of the ellipsometer light source. Therefore, $(V/V_e)^n$ is a measure of the reduction of the ellipsometer signal due to sample emission. Over most of the spectrum it was not necessary to correct the measurements since values of $V_e \gtrsim 1000$ V and $V \leq 600$ V were measured, and for the eleven-stage phototube this implies a signal reduction less than or equal to 4×10^{-3} . This was true for all but the blue end of the spectrum of the 700°C measurement. A correction was made for this spectrum by running two additional scans: one with a uv band-pass filter in front of the phototube (effectively eliminating all sample emission), and one without the uv band-pass filter. This procedure resulted in a small (less than 10%) correction to the data.

Sample temperature was measured by a Chromel-Alumel thermocouple in direct contact with the back of the wafer. To increase the thermal contact between the sample and the substrate heater, a graphite suspension was used between the sample and the heating block and the thermocouple. Since the forming gas flowing over the sample was preheated by the heater block and the sample chamber was totally enclosed (with the exception of the two small optical ports), sample temperature reduction due to heat exchange with the forming gas and to sample emission was nearly eliminated, and the thermocouple measured the actual sample temperature. The temperature of the heater was controlled to $\pm 7^\circ\text{C}$.

The optical functions were obtained from the ellipsometric data using the effective-oxide-thickness approximation (see Refs. 12 and 27); the primary uncertainty is in the value of the oxide thickness. The effective oxide thickness was 17 Å for temperatures less than or equal to 400°C and increased to

$\sim 27 \text{ \AA}$ for the 700°C measurement. The actual value of the oxide thickness of the high-temperature measurements was determined by a comparison with before and after low-temperature ellipsometry measurements. We determined that the error in the oxide thickness was less than 2 \AA for the 600 and 700°C data sets, and less than 0.5 \AA for the other data sets. A detailed examination of the error in the dielectric functions of silicon introduced by errors in the angle of incidence, the ellipsometry parameters ψ and Δ , and the oxide thickness is given in Ref. 12. Using a similar analysis, we conclude that the error in ϵ_1 and ϵ_2 is less than 1.5 and is dependent upon photon wavelength. For photon energies well below the direct band gap, the error in ϵ_2 is determined by the oxide thickness and Δ , and it decreases to less than 0.1, while the error in $\epsilon_1 \sim 0.3$ and is determined mostly by errors in the angle of incidence and ψ .

III. RESULTS AND DISCUSSION

The resulting values of the dielectric functions are shown in Fig. 1 as a function of wavelength for several temperatures. The following features of Fig. 1 are immediately apparent.

(1) The peak in ϵ_2 near 4.4 eV at 10 K decreases in magnitude and moves to lower energy as the temperature increases. The zero crossing of the ϵ_1 spec-

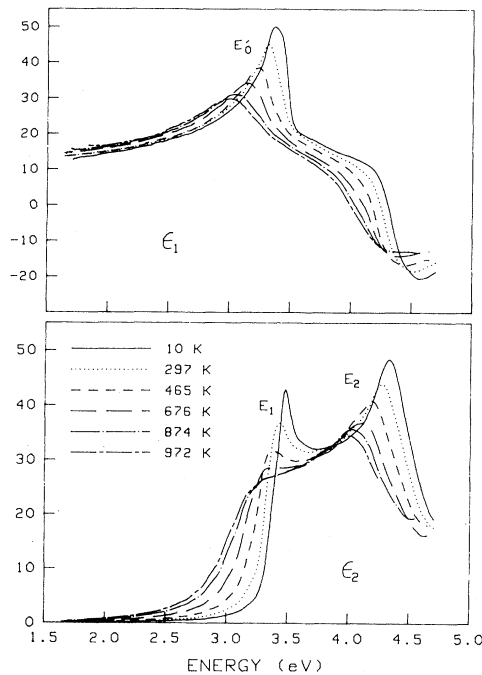


FIG. 1. Real and imaginary parts of the dielectric function of silicon for several temperatures.

trum occurs at nearly the same energy, and the slope decreases with increasing temperature. This peak in ϵ_2 has been labeled E_2 in Fig. 1; its origin is not clear, but it is thought to be due to several critical points, including the transitions $\Sigma_2^v \rightarrow \Sigma_3^c$.²⁹ None of these features are resolved at higher temperatures.

(2) The peak in ϵ_1 near 3.4 eV at 10 K also decreases in magnitude, moves to lower energy, and broadens as the temperature increases; it is manifested in the ϵ_2 spectra as a low-energy cutoff shoulder. This peak is labeled E'_0 in Fig. 1 and is thought to arise primarily from an M_0 critical point in the joint density of states for the $\Gamma_{25}^v \rightarrow \Gamma_{15}^c$ transition.¹⁰ Daunois and Aspnes¹⁰ found that the critical-point energy for this transition did not occur exactly at the top of the peak but rather at the low-energy side.

(3) The peak in ϵ_2 near 3.4 eV at 10 K decreases in magnitude and moves to lower energy as the temperature is increased until it is no longer observable at $\sim 500^\circ\text{C}$. A high-energy cutoff shoulder in the ϵ_1 spectrum at the same energy is observable upon close examination of the 10-K data. This peak is labeled E_1 in Fig. 1 and corresponds to either a M_0 or M_1 critical point for the $\Lambda_3^v - \Lambda_1^c$ transition.¹⁰ As with E'_0 , Daunois and Aspnes¹⁰ found that the critical-point energy at 10 and 300 K is at slightly lower energy than the peak position. The disappearance of this peak is probably due to the fact that E_1 moves to lower energy faster than E'_0 , and once the E_1 peak is lower in energy than the E'_0 shoulder it will not be unobservable.

As a result of these movements, ϵ_2 is nearly independent of temperature from 3.8 to 3.2 eV above $\sim 500^\circ\text{C}$. A plot of α vs $h\nu$ for several temperatures indicates that $\alpha(\lambda, T)$ also becomes independent of T above a critical wavelength $\lambda_c(T)$. An empirical fit to this saturation value of α in the vicinity of 3.4 eV yields $\alpha = \alpha_0 \exp(h\nu/E_0)$, where $\alpha_0 = 4.1 \times 10^4 \text{ cm}^{-1}$ and $E_0 = 1.09 \text{ eV}$. By examining the 500, 600, and 700°C $\alpha(\lambda)$ spectra, it appears that λ_c moves monotonically to a longer wavelength with increasing temperature. Therefore, it is reasonable to expect the above expression to yield the asymptotic value for α at temperatures higher than 700°C .

(4) As the temperature is increased, all features become broadened. This is due primarily to the increased phonon population at elevated temperatures, which relaxes somewhat the requirement of strict k conservation.

(5) Below the E_1 and E'_0 features, ϵ_2 increases monotonically with temperature. For photon energies well below 3.4 eV and for temperatures between 300 and 1000 K, the absorption coefficient, which is related to ϵ_2 , obeys the empirical relation²⁷

$$\alpha(\lambda, T) = \alpha_0(\lambda) \exp(T/T_0), \quad (3)$$

where $T_0=430^\circ\text{C}$ for all photon energies, and the prefactor $\alpha_0(\lambda)$ is a function of photon wavelength. Equation (3) only holds when the photon energy is well below the E_1 and E'_0 features; for photon energies near this peak, a more complicated behavior is observed. Initially, α increases exponentially, as in Eq. (3), but as the E_1 and E'_0 features approach the photon energy in question, α then approaches asymptotically the limit given in (3) above.

The temperature dependence of the normal-incidence reflectance was determined from the optical functions and is shown in Fig. 2. As can be seen, the peak in R near 3.4 eV at 10 K moves to lower energies with increasing temperature, and disappears around 500°C . Above 500°C , R is a monotonically increasing function of energy from 2 to 4 eV. Below ~ 3 eV, R increases linearly with temperature, and is given by

$$R(\lambda, T) = R_0(\lambda, T = 300 \text{ K}) + 5 \times 10^{-5} T, \quad (4)$$

with T in units of K.

All previous ellipsometric determinations of the optical function of silicon as a function of temperature were performed with single-wavelength (632.8 nm) nulling ellipsometers¹³⁻¹⁵; these data are shown in Fig. 3. van der Meulen and Hien¹⁵ performed measurements in pure N_2 up to 1350 K on substrates that were intentionally oxidized with a thin (less than 175 Å) layer of SiO_2 . The two samples of Hopper *et al.*¹⁴ were first heated to 1200°C for ~ 30 sec in 10^{-7} Torr to remove oxide on the sample sur-

face, and then intentionally oxidized to (1) 18 Å and (2) 2810 Å before the measurements, which were carried out in vacuum. In contrast, Algazin *et al.*¹³ prepared atomically pure silicon surfaces by vacuum-high-temperature refining at a temperature of $1250-1300^\circ\text{C}$.

The data from our work at 632.8 nm are also shown in Fig. 3 for comparison. The principal sources of error in our measurements at 632.8 nm are (1) errors in ψ and in the angle of incidence ϕ for ϵ_1 ; and (2) errors in Δ and in the oxide thickness for ϵ_2 . The resulting confidence limits at 700°C for our data are shown in Fig. 2; these confidence limits are determined from the error matrix shown in Table I, assuming $\Delta\phi=0.2^\circ$, $\Delta d=2.0$ Å, $\Delta\psi=0.1^\circ$, and $\Delta(\Delta)=0.1^\circ$. As can be seen, our data for ϵ_1 and ϵ_2 are in general agreement with the data sets of van der Meulen and Hien¹⁵ and of Hopper *et al.*¹⁴ The principal disagreement comes with the data set of Algazin *et al.*¹³; this discrepancy could be due to sample preparation, in that the refining technique of Algazin *et al.*¹³ could have resulted in a large number of defects in the near-surface region, thereby generally increasing ϵ_2 for all temperatures. Another possibility is that a small amount of oxide growth could have occurred during the measurement; if this were not properly taken into account, a larger value of ϵ_2 would be determined (a 10-Å growth would be sufficient to explain the discrepancy). Algazin *et al.*¹³ attribute the discrepancy between their data and the data sets of Refs. 14 and 15 as being due to

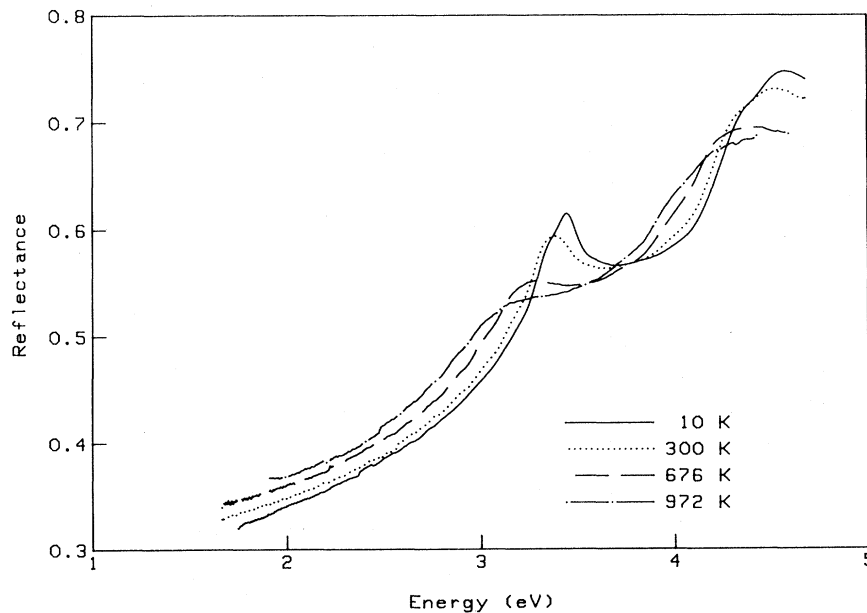


FIG. 2. Normal incidence reflectance of Si at several selected temperatures.

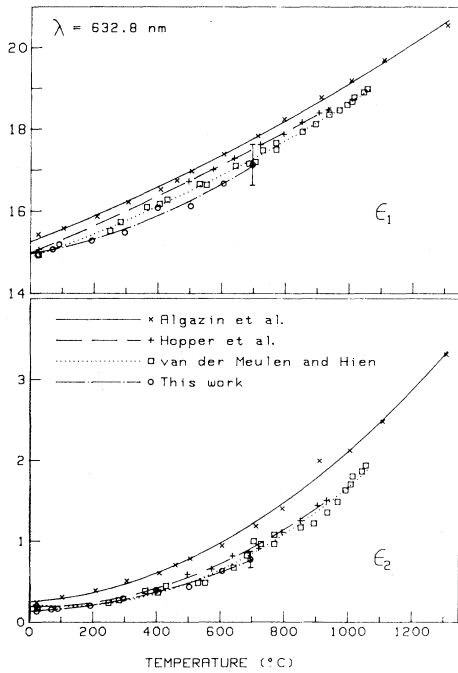


FIG. 3. Optical functions at elevated temperatures from this work compared with the data in the literature: Algazin *et al.* (Ref. 13), Hopper *et al.* (Ref. 14), and van der Meulen and Hien (Ref. 15).

the presence of an interface layer between Si and SiO₂. However, Jellison and Modine³⁰ have shown that reasonable interface layers between Si and SiO₂ cannot change ψ and Δ appreciably at this wavelength. Therefore no discrepancy should exist if the oxide layer is properly taken into account.

The absorption coefficient of silicon has been measured by Weakliem and Redfield¹⁶ up to 200°C using transmission measurements. Their data set agrees with our data at low photon energies, but deviates significantly at high temperatures and/or high photon energies such that $\alpha \gtrsim 5 \times 10^3$, with their α data being lower than ours. Similar observations can be made when comparing our data and

TABLE I. Comparison of the errors introduced into the determination of ϵ_1 and ϵ_2 at 632.8 nm by the angle of incidence (ϕ), the oxide thickness (d), and the ellipsometric parameters ψ and Δ . The two-boundary approximation has been used.

Error	$\Delta\epsilon_1$	$\Delta\epsilon_2$
$\Delta\phi = 0.1^\circ$	0.162	-0.006
$\Delta d = 0.5 \text{ \AA}$	0.000	-0.027
$\Delta\psi = 0.1^\circ$	0.111	0.008
$\Delta(\Delta) = 0.1^\circ$	0.002	-0.027

that of Compaan and Lo,¹⁸ which was taken using very thin silicon-on-sapphire samples and optical transmission measurements. In all cases, the transmission measurements result in lower values of α than do the ellipsometric measurements. This has been discussed in Ref. 12 with respect to room-temperature measurements, where it was concluded that the discrepancies were due to the difficulties associated with obtaining very thin defect-free samples with optically polished surfaces. The difficulty of comparing with the result of Compaan and Lo¹⁸ is compounded by the fact that their samples were silicon on sapphire, which can have considerably different optical properties from bulk Si.¹²

As was stated in (4) above, the features of ϵ_1 and ϵ_2 become broadened as the temperature is increased. Nevertheless, it is possible to determine the temperature dependence of the E'_0 and E_2 features by plotting their peak positions as a function of temperature; this is done in Fig. 4. (Because the E'_0 peak in ϵ_1 does not correspond directly to the position of the critical point in the joint density of states,¹⁰ a small temperature-dependent error may be introduced in the determining position of the E'_0 peak from the dielectric spectra.) The best fit of this data to the empirical relation of Varshni,²⁸

$$E(T) = E(0) - \frac{\alpha T^2}{T + \beta}, \quad (5)$$

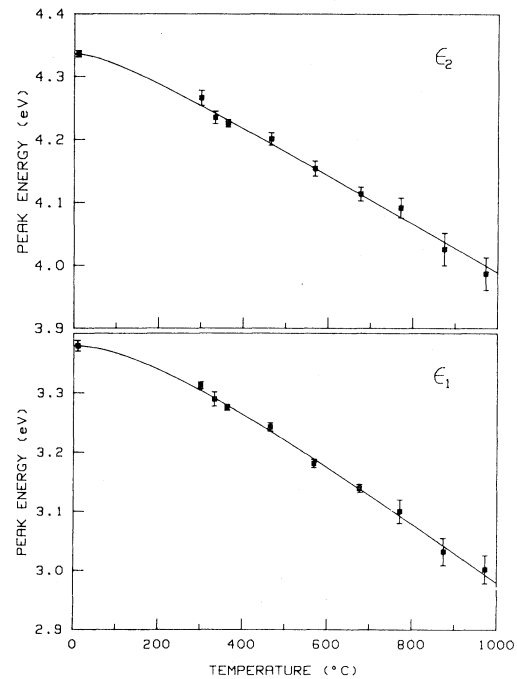


FIG. 4. Energy position of the peak in ϵ_1 and ϵ_2 as a function of temperature. Solid lines through the data represent a least-squares fit to the data using Eq. (5) with parameters given in Table II.

was determined. A linear least-squares-fitting procedure similar to that of Thurmond³¹ was used to determine the constants α , β , and E_0 , which are shown in Table II. The solid lines of Fig. 4 are determined using Eq. (5) and the appropriate constants of Table II. As can be seen from Table II, all three gaps yield approximately the same value of α (within experimental error), but the values of β are quite different. Other thermodynamic functions for the formation of electrons and holes can be calculated from Eq. (5) using familiar thermodynamic relationships.³¹ The gap entropy $S(T)$, change in enthalpy $H(T)-H(0)$, and the specific heat $C(T)$ are given by

$$S(T) = \frac{\alpha T(T+2\beta)}{(T+\beta)^2}, \quad (6a)$$

$$H(T)-H(0) = \frac{\alpha\beta T^2}{(T+\beta)^2}, \quad (6b)$$

and

$$C(T) = \frac{2\alpha\beta^2 T}{(T+\beta)^3}. \quad (6c)$$

The values of $S(T)$, $H(T)-H(0)$, $E(T)-E(0)$, and $C(T)$ are shown in Fig. 5, where $S(T)$ and $C(T)$ have been normalized by Boltzmann's constant, and H and E are expressed in eV. As can easily be seen, there is a significant difference in the thermodynamic properties of the three gaps; however, Van Vechten and Thurmond's³³ argument that the entropy of electron-hole pair formation for all gaps in a semiconductor is the same to within a factor of 2 appears to be valid above ~ 300 K.

Calculations of the temperature dependence of the E_1 , E_0 , and E_2 gaps, as well as the indirect gap of silicon have recently been performed by Mostoller,³⁴ where the temperature dependence was incorporated via the Debye-Waller factor and linear expansion of the lattice. The calculated changes of the energy gaps with temperature were all much larger than the observed changes. This result is consistent with the results of Allen and Cardona,²⁶ where they found that simply including the temperature dependence of the E_0 band gap of Ge via the Debye-Waller factor resulted in a large discrepancy between theory and

TABLE II. Constants of Eq. (4).

Gap	Energy at $T=10$ K	α (10^{-4} eV K $^{-1}$)	β (K $^{-1}$)
Indirect	1.170 ^a	4.73 ± 0.25^b	636 ± 50^b
Direct E_2	4.330	3.91 ± 0.43	125 ± 65
Direct E'_0	3.378	5.37 ± 0.82	342 ± 110

^aReferences 32 and 17.

^bReference 31.

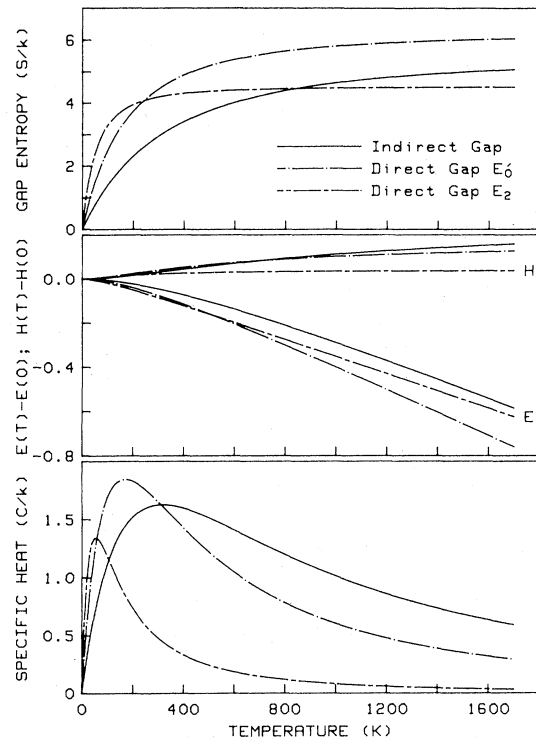


FIG. 5. Thermodynamic functions vs temperature determined from Eqs. (5) and (6) using the values of the parameters in Table II. Gap entropy (S) and specific heat (C) are given in units of Boltzmann's constant k , while the gap energy (E) and the enthalpy (H) are given in eV.

experiment; the inclusion of the self-energy term improved the agreement, but it still was not good. This is contrasted to the results of Walter *et al.*³⁵ where they found that the simple inclusion of the Debye-Waller factor was sufficient to get good agreement between theory and experiment for the E_1 doublet and the E_2 peak in GaAs. Clearly, more calculations are required to get good agreement between theory and experiment in Si and Ge, and to ensure that the self-energy term is negligible in GaAs. It is hoped that this data will stimulate such calculations.

ACKNOWLEDGMENTS

The authors acknowledge M. Mostoller for performing the temperature-dependent energy-gap calculations of Si and for many helpful discussions. The authors also acknowledge D. H. Lowndes and D. E. Aspnes for carefully reading this manuscript. This research was sponsored by the Division of Materials Sciences, U. S. Department of Energy under Contract No. W-7405-eng-26 with the Union Carbide Corporation.

- ¹R. F. Wood, D. H. Lowndes, and G. E. Giles, in *Laser and Electron Beam Interactions with Solids*, edited by B. R. Appleton and G. K. Celler (North-Holland, New York, 1982), p. 67; R. F. Wood, M. Rasolt, and G. E. Jellison, Jr. *ibid.*, p. 61.
- ²S. M. Vernon and W. A. Anderson, *Appl. Phys. Lett.* **26**, 707 (1975); B. Bhaumik and R. Sharon, *ibid.* **29**, 257 (1976).
- ³H. W. Lo and A. Compaan, *Phys. Rev. Lett.* **40**, 1604 (1980); A. Compaan, A. Aydinli, M. C. Lee, and H. W. Lo, in *Laser and Electron Beam Interactions with Solids*, edited by B. R. Appleton and G. K. Celler (North-Holland, New York, 1982), p. 43.
- ⁴J. B. Renucci, R. N. Tyte, and M. Cardona, *Phys. Rev. B* **11**, 3885 (1975).
- ⁵G. E. Jellison, Jr., D. H. Lowndes, and R. F. Wood, in *Laser and Electron Beam Interactions with Solids*, edited by W. L. Brown and J. Narayan (North-Holland, New York, in press).
- ⁶W. C. Dash and R. Newman, *Phys. Rev.* **99**, 1151 (1955).
- ⁷H. R. Phillip, *J. Appl. Phys.* **43**, 2835 (1972).
- ⁸H. R. Phillip and E. A. Taft, *Phys. Rev.* **120**, 37 (1960).
- ⁹H. R. Phillip and H. Ehrenreich, *Phys. Rev.* **129**, 1550 (1963).
- ¹⁰A. Daunois and D. E. Aspnes, *Phys. Rev.* **18**, 1824 (1978).
- ¹¹D. E. Aspnes and J. B. Theeten, *J. Electrochem. Soc.* **127**, 1359 (1980).
- ¹²G. E. Jellison, Jr. and F. A. Modine, *J. Appl. Phys.* **53**, 3745 (1982).
- ¹³Yu. B. Algazin, Yu. A. Blyumkina, N. I. Grebnev, K. K. Svitashv, L. V. Semenenko, and T. M. Yablontseva, *Opt. Spectrosc.* **45**, 183 (1978).
- ¹⁴M. A. Hopper, R. A. Clark, and L. Young, *Electrochem. Soc.* **122**, 1216 (1975).
- ¹⁵Y. J. van der Meulen and N. C. Hien, *J. Opt. Soc. Am.* **64**, 804 (1974).
- ¹⁶H. A. Weakliem and D. Redfield, *J. Appl. Phys.* **50**, 1491 (1979).
- ¹⁷G. G. Macfarlane, T. P. McLean, J. E. Quarrington, and V. Roberts, *Phys. Rev.* **111**, 1245 (1958).
- ¹⁸A. Compaan and H. W. Lo, in *Laser and Electron Beam Processing of Materials*, edited by C. W. White and P. S. Peercy (Academic, New York, 1980), p. 11.
- ¹⁹G. E. Jellison, Jr. and D. H. Lowndes, *Appl. Phys. Lett.* **41**, 594 (1982).
- ²⁰M. L. Cohen and D. J. Chadi, in *Handbook on Semiconductors*, edited by M. Balkanski (North-Holland, New York, 1980), Vol. 2, Chap. 4B.
- ²¹H. Y. Fan, *Phys. Rev.* **82**, 900 (1951).
- ²²E. Antonchik, *Czechoslov. J. Phys.* **5**, 449 (1955).
- ²³H. Brooks and S. C. Yu (unpublished); S. C. Yu, Ph.D. thesis, Harvard University, 1967 (unpublished).
- ²⁴H. Brooks, *Adv. Electron.* **7**, 85 (1955).
- ²⁵V. Heine and J. A. Van Vechten, *Phys. Rev. B* **13**, 1622 (1976).
- ²⁶P. B. Allen and M. Cardona, *Phys. Rev. B* **23**, 1495 (1981); **24**, 7479 (1981).
- ²⁷G. E. Jellison, Jr. and F. A. Modine, *Appl. Phys. Lett.* **41**, 180 (1982).
- ²⁸Y. P. Varshni, *Physica* **34**, 149 (1967).
- ²⁹K. Kondo and A. Moritani, *Phys. Rev. B* **15**, 812 (1977).
- ³⁰G. E. Jellison, Jr. and F. A. Modine, *J. Opt. Soc. Am.* **72**, 1253 (1982).
- ³¹C. D. Thurmond, *J. Electrochem. Soc.* **122**, 1133 (1975).
- ³²W. Bludau, A. Onton, and W. Heinke, *J. Appl. Phys.* **45**, 1846 (1974).
- ³³J. A. Van Vechten and C. D. Thurmond, *Phys. Rev. B* **14**, 3539 (1976).
- ³⁴M. Mostoller (private communication).
- ³⁵J. P. Walter, R. F. L. Zucca, M. L. Cohen, and Y. R. Shen, *Phys. Rev. Lett.* **24**, 102 (1970).